



Title	CW transillumination imaging by extracting weakly scattered light from strongly diffused light
Author(s)	Takagi, Kazuto; Kakinuma, Hiroyuki; Kato, Yuji; Shimizu, Koichi
Citation	Optics Express, 17(10), 8332-8342
Issue Date	2009-05-11
Doc URL	http://hdl.handle.net/2115/38631
Rights	© 2009 Optical Society of America, Inc.
Type	article
File Information	17-10_p8332-8342.pdf



[Instructions for use](#)

CW transillumination imaging by extracting weakly scattered light from strongly diffused light

Kazuto Takagi,* Hiroyuki Kakinuma, Yuji Kato, and Koichi Shimizu

Graduate School of Information Science and Technology, Hokkaido University,
N 14 W 9, Kita-ku, Sapporo, 060-0814 Japan

*Corresponding author: k-takagi@bme.ist.hokudai.ac.jp

Abstract: Transmitted light through a diffuse scattering medium includes strongly diffused light (SDL) and weakly scattered light (WSL). To realize clear transillumination imaging through thick body tissue, which is typically more than 10 mm, we developed a technique to extract the WSL component from diffused light. In experiments using a 15-mm-thick scattering medium ($\mu_s' = 1.0/\text{mm}$), the cross-section of the light propagation area at the center of the medium was confined to a 50% area. This method's usefulness was demonstrated by transillumination imaging through a 40-mm-thick piece of chicken meat. The possibility of depth evaluation was also verified.

©2009 Optical Society of America

OCIS codes: (290.1990) Diffusion; (290.4210) Multiple scattering; (290.5839) Scattering, invisibility; (170.3660) Light propagation in tissues.

References and links

1. S. G. Demos and R. R. Alfano, "Optical polarization imaging," *Appl. Opt.* **36**, 150–155 (1997).
2. S. G. Demos, H. B. Radousky, and R. R. Alfano, "Deep subsurface imaging in tissues using spectral and polarization filtering," *Opt. Express* **7**, 23–28 (2000).
3. Stephen P. Morgan, Man P. Khong, and Michael G. Somekh, "Effects of polarization state and scatterer concentration on optical imaging through scattering media," *Appl. Opt.* **36**, 1560–1565 (1997).
4. M. A. Franceschini, K. T. Moesuta, S. Fantini, G. Gaida, E. Gratton, H. Jess, W. W. Mantulin, M. Seever, P. M. Schlag, and M. Kaschke, "Frequency-domain techniques enhance optical mammography: Initial clinical results," *Proc. Natl. Acad. Sci. USA* **94**, 6468–6473 (1997).
5. S. Fantini, S. A. Franceschini, G. Gaida, E. Gratton, H. Jess, W. W. Mantulin, K. T. Moesta, P. M. Schlag, and M. Kaschke, "Frequency-domain optical mammography: Edge effects correction," *Med. Phys.* **23**, 149–157 (1996).
6. D. Grosenick, H. Wabnitz, H. H. Rinneberg, K. T. Moesta, and P. M. Schlag, "Development of a time-domain optical mammograph and first in-vivo applications," *Appl. Opt.* **38**, 2927–2943 (1999).
7. D. Grosenick, K. T. Moesta, H. Wabnitz, J. Mucke, C. Stroszcynski, R. Macdonald, P. M. Schlag, and H. H. Rinneberg, "Time-domain optical mammography: initial clinical results on detection and characterization of breast tumors," *Appl. Opt.* **42**, 3170–3186 (2003).
8. D. Grosenick, H. Wabnitz, and H. Rinneberg, "Time-resolved imaging of solid phantoms for optical mammography," *Appl. Opt.* **36**, 221–231 (1997).
9. A. O. Wist, P. P. Fatouros, and S. L. Herr, "Increased spatial resolution in transillumination using collimated light," *IEEE Trans. Med. Imaging* **12**, 751–757 (1993).
10. S. Tanosaki, M. Takagi, Y. Sasaki, A. Ishikawa, H. Inage, R. Emori, J. Suzuki, T. Yuasa, H. Taniguchi, B. Devaraj, and T. Akatsuka, "*In vivo* laser tomographic imaging of mouse leg with coherent detection imaging method," *Opt. Rev.* **10**, 447–451 (2003).
11. K. Shimizu, and M. Kitama, "Fundamental study on near-axis scattered light and its application to optical computed tomography," *Opt. Rev.* **7**, 383–388 (2000).
12. K. Takagi, Y. Kato, and K. Shimizu, "CW detection of near-axis scattered light for transillumination imaging," in *Biomedical Optics Topical Meeting*, Technical Digest (CD) (Optical Society of America, 2006), paper SH67.

1. Introduction

Transillumination imaging using near-infrared light is useful for noninvasive measurement of animal bodies. However, severe light scattering occurring in biological tissues blurs a transilluminated image. Many techniques have been proposed to suppress this scattering effect. Deep tissue imaging techniques using cross-polarization and multiwavelength light sources have been proposed for transillumination imaging using backscattered light [1, 2]. A technique subtracting cross-polarization from parallel-polarization has been proposed to improve the spatial resolution of transillumination imaging [3]. In addition, frequency domain techniques [4, 5] and time domain techniques [6–8] have been proposed for optical mammography. However, these techniques require complex and/or large devices. Among scattering suppression techniques, CW techniques are useful in practice because of their simplicity and stability of measurement. For example, techniques to detect ballistic photons [9, 10] and near-axis scattered light (NASL) [11, 12] have been reported based on these practical advantages. However, ballistic photons can reach the detector across body tissues of only a few millimeters' thickness, and NASL can reach the detector after penetrating body tissues of about 10 millimeters' thickness. Although these techniques provide high spatial resolution, they are applicable only to very thin parts of the body.

Herein, we propose a new technique that provides transillumination images of body parts for which conventional CW techniques are ineffective. This technique resembles the NASL extraction technique we reported before [12]. In the previous technique, we differentiated the NASL component by the difference of photon propagation paths in a scattering medium. Consequently, the use of an optical collimation system was necessary. This makes the received light intensity rapidly undetectable as the body part thickness increases to more than 10 mm. In the new technique, we differentiate the WSL component by the degree of diffusion. It requires no collimation system. Therefore, we can expect a much larger signal-to-noise ratio in the received light intensity and larger applicable thickness of body parts.

As described in this paper, we present the principle of the proposed technique and verify its feasibility in experiments. The effectiveness of the proposed technique is demonstrated in the measurement of the propagation area of the received WSL component in a scattering medium. In addition to presenting results of transillumination imaging through a model phantom and biological tissues, we describe the possibility of depth evaluation of absorbers in a scattering medium as an application of this technique.

2. Principle of WSL extraction

First, we consider the case in which the optical density of the scattering medium is small, $\mu_s' L < 10$, where μ_s' and L respectively signify the reduced scattering coefficient and the geometrical thickness of the scattering medium. In this case, light components of three kinds are in the transmitted light on the other side of the medium when we illuminate a beam of light on one side of the scattering medium. They are the ballistic, the NASL, and the diffused light components. Here, the term "diffused light component" is defined as a scattered light component except for the NASL component. Figure 1 schematically presents the propagation areas of these light components in a scattering medium in the case of point incidence – point detection. The ballistic light component propagates on the optical axis. The NASL component propagates in the near-axis region. The spread of its propagation area is approximately constant at all depths. However, the diffused light component propagates in the off-axis region.

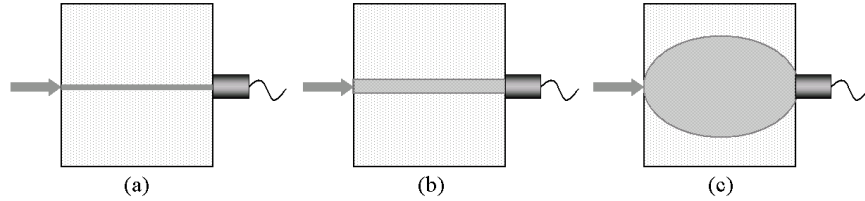


Fig. 1. Propagation area in a scattering medium: (a) ballistic component, (b) NASL component, (c) diffused light component.

The ballistic light component decreases rapidly when the optical density of the scattering medium increases. The attenuation rate of the NASL is smaller than that of the ballistic light component when the optical density of the scattering medium increases. However, the NASL component is hardly present in the transmitted light when the optical density $\mu_s L$ of the scattering medium becomes greater than 10. Therefore, the transmitted light practically consists of only a diffused light component when a scattering medium has optical density greater than 10. In this case, the transillumination image is blurred severely. Consequently, it has been believed that clear imaging is hardly possible with such a medium. Although diffused light propagates in a wide area of the scattering medium, the WSL component in the diffused light propagates in a much narrower area. Therefore, we could expect clear transillumination imaging if we were able to extract the WSL component selectively from the diffused light. However, direct detection of the WSL component is not easy. In the proposed technique, the WSL component is extracted by subtracting the SDL component from the transmitted diffused light.

Figure 2(a) shows the case in which the optical density of the scattering medium is comparatively large: $\mu_s L > 10$. We define the spatial intensity distribution of the transmitted light in this case as $I_1(x, y)$. Next, we install a diffuser plate on the incident side of the scattering medium, as presented in Fig. 2(b). We define the spatial intensity distribution of the transmitted light in this case as $I_2(x, y)$. The incident light is deflected to random directions by the diffuser, and the WSL component in the transmitted diffused light component is reduced, as presented in Fig. 2(b). However, the off-axis intensity does not change as much as the near-axis intensity because of the strong diffuse scattering in the scattering medium. The change in the WSL component is dominant in the change of output light through the scattering medium. Therefore, we can extract the WSL component $I_{WSL}(x, y)$ by subtracting $I_2(x, y)$ from $I_1(x, y)$ with an appropriate weight α , as

$$I_{WSL}(x, y) = I_1(x, y) - \alpha I_2(x, y). \quad (1)$$

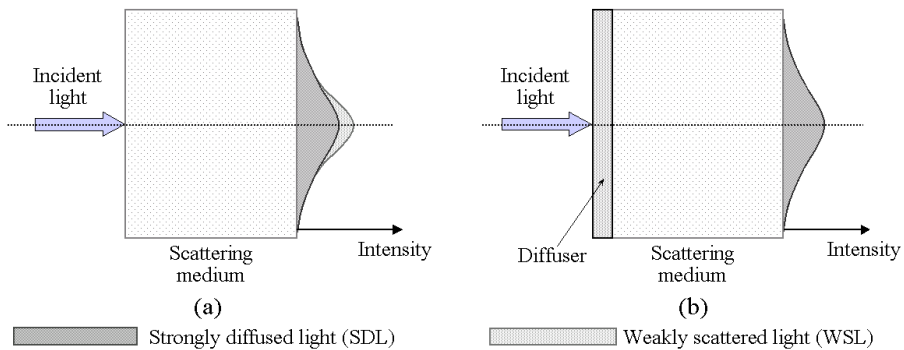


Fig. 2. Principle to extract weakly scattered light: (a) without diffuser, (b) with diffuser.

3. Validity test of proposed principle

The validity of the proposed technique was tested in experiments. The spatial and temporal spreads of a light after passing through a scattering medium are measured. Both spreads of the extracted light are expected to be smaller than those of diffusely transmitted light if we can extract the WSL component correctly. The spatial spread of a light beam after passing through a scattering medium was evaluated in a CW measurement. The temporal spread of a short pulse of light was also evaluated in a time-resolved measurement.

3.1 Spatial distribution of scattered light

Figure 3 shows the experimental setup schematically. As a scattering medium, an aqueous solution of Intralipid (reduced scattering coefficient $\mu_s' = 1.0/\text{mm}$) was used in an acrylic resin container with the inner wall separation of 15 mm along the optical axis of the incident light beam. As a light source and a diffuser, a CW Ti:Sapphire laser (750 nm wavelength) and one side frosted diffuser (BK7, # 600) were used, respectively.

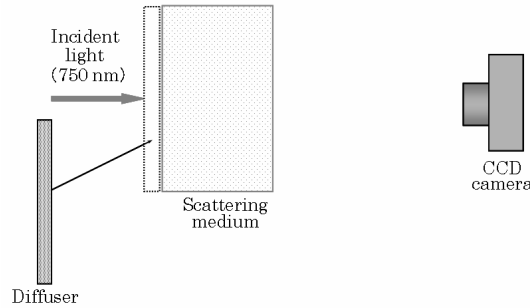


Fig. 3. Experimental setup to extract weakly scattered light in CW measurement.

In the first process, a laser light beam ($1.4 \text{ mm}\phi$) was illuminated on the scattering medium. The intensity distribution at the output surface $I_1(x, y)$ was recorded using a cooled CCD camera. In the second process, the diffuser was placed on the incident side of the scattering medium. Using the same system as that used in the first process, the intensity distribution of the transmitted light $I_2(x, y)$ was recorded. Consequently, the image of the WSL component was obtained as shown in Eq. (1). Here, the subtraction weight α was determined as 1.1 according to the ratio of I_1 to I_2 at 15 mm from the optical axis.

Figures 4(a)–4(c) respectively present $I_1(x, y)$, $I_2(x, y)$, and $I_{\text{WSL}}(x, y)$. The intensity distributions along the sampling lines (white broken lines) of Figs. 4(a)–4(c) are presented in Fig. 5. The intensity distributions of Fig. 5 were normalized by the maximum value of Fig. 4(a). The full width at half maximum of the beam spread in the original case was 19.2 mm. It decreased to 13.6 mm by the proposed technique. This result corresponds to an approximately 50% reduction of the cross sectional area.

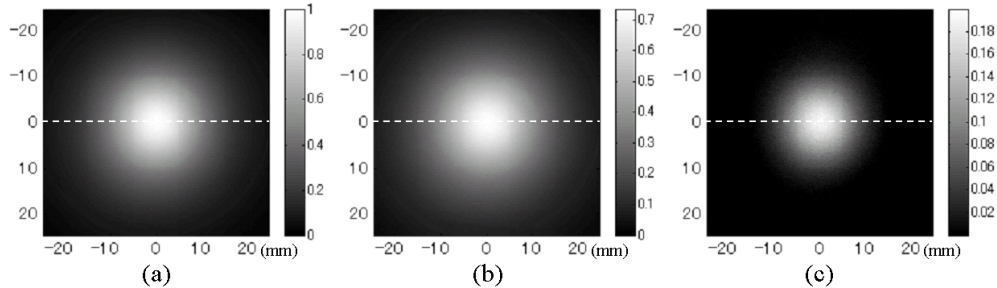


Fig. 4. Images through scattering medium ($\mu_s' L = 15$): (a) without diffuser, (b) with diffuser, (c) subtracted image.

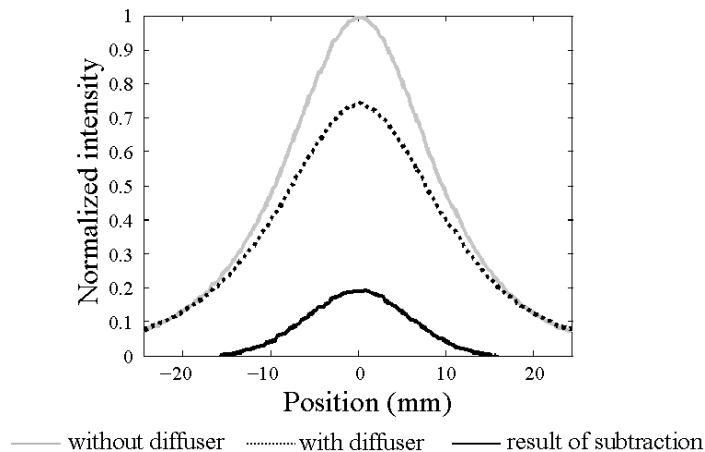


Fig. 5. Intensity distributions along white broken lines in Figs. 4(a)–4(c).

3.2 Temporal distribution of scattered light

The temporal spread of a short pulse of light was measured to examine the effectiveness of the proposed technique. The measurement system was identical to that described in section 3.1, except for the following points. As a light source and detector, a mode-locked Ti:Sapphire laser (800 nm wavelength, 20 ps pulse width, 76 MHz repetition rate) and a streak camera (20 ps temporal resolution) were used, respectively. The light pulse was illuminated on the scattering medium. The transmitted light on the optical axis of incident light beam was led to the streak camera by an optical fiber with 200 μm core diameter. The temporal distribution of the WSL component was obtained by subtracting the pulse shape after the diffuser placement from that before the diffuser placement. The subtraction weight α was 1.1, which is the same as that reported in section 3.1.

Figure 6 presents results of the time-resolved measurement. The time region of the half maximum of the pulse shape before the diffuser placement spreads over a later time, 230–620 ps. On the other hand, that of the subtracted pulse shape spreads over 190–480 ps. The earlier time component with a smaller temporal spread was extracted successfully using the proposed technique. These results of spatial and temporal measurements show that we can extract the WSL component from widely diffused light using the proposed technique.

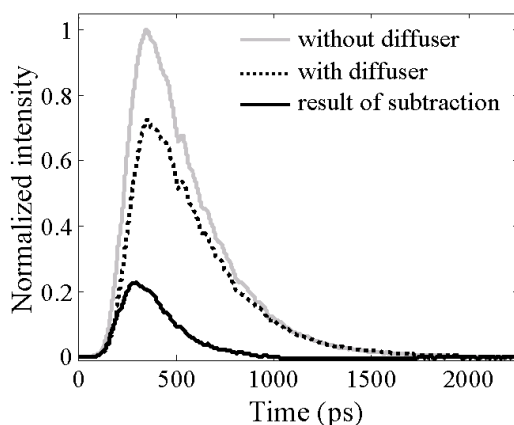


Fig. 6. Temporal profiles of transmitted light through a scattering medium.

4. Measurement of propagation area

The spatial resolution of transillumination imaging depends strongly on the narrowness of the propagation area of the incident light beam in the scattering medium. The propagation area of the detected WSL component was measured to examine the effectiveness of the proposed technique. The measurement was based on beam profiling with a knife-edge plate. Figure 7 presents the sample part of the experimental setup schematically. The measurement system resembles that described in section 3.1, except for the following point. As a detector, a PIN photodiode with a scanning mechanism was used instead of the CCD camera for better quantitative analysis. The cross section of the incident beam was a circle. We therefore assumed cylindrical symmetry for light propagation in a scattering medium. First, a knife-edge plate was placed perpendicular to the optical axis at the position to obstruct all light. Then, by shifting the knife-edge plate up across the optical beam by distance x , as presented in Fig. 8(a), the transmitted intensity I was measured as a function of x , as presented in Fig. 8(b). The derivative (dI/dx) gives the light distribution in the cross sectional plane of the plate. The spread of the propagation path of the detected light was evaluated as the beam width of the measured profile of the light distribution.

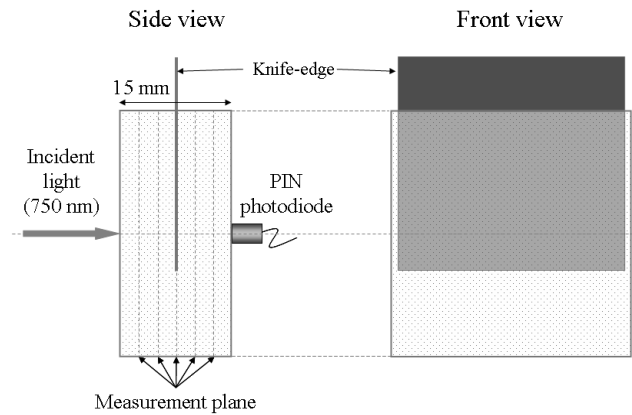


Fig. 7. Experimental setup to measure propagation area.

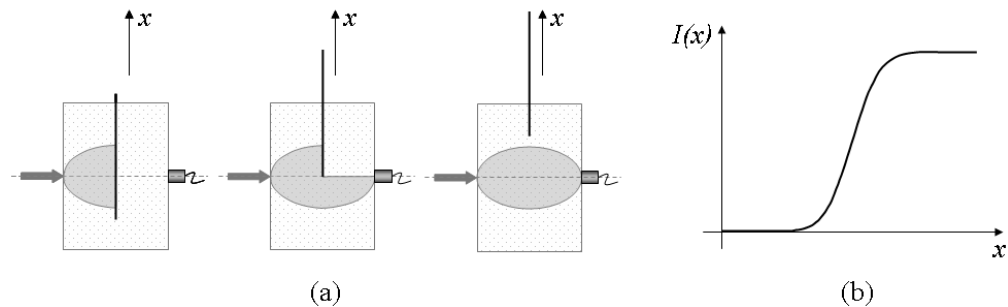


Fig. 8. Schematic diagram of measurement procedure: (a) movement of knife-edge plate, (b) measured transmitted intensity.

The incident beam diameter was 1.4 mm; the subtraction weight $\alpha=1.0$ was determined by the intensity at the off-axis area 15 mm from the optical axis. The profile was measured in the vertical plane perpendicular to the horizontal optical axis. Positions of the measurement plane were 2.5, 5.0, 7.5, 10.0, and 12.5 mm distant from the incident surface of the 15-mm-thick scattering medium.

Figure 9(a) presents results of the measurement at the plane 7.5 mm far from the incident surface. The slow increase of transmitted light attributable to a scattering effect was improved using the proposed technique. The beam width in a scattering medium was defined as the width between the 12% and 88% points of the intensity change presented in Fig. 9(a). This width corresponds to the full width at half maximum if the intensity distribution is assumed as a two-dimensional Gaussian distribution. Figure 9(b) depicts the spread of the propagation paths of the detected light along the optical axis. The optical density of the scattering medium in this case was $\mu_s' L = 15$. The propagation paths of the WSL component detected by the proposed technique were confined to smaller widths at all depths. The cross sectional area at 7.5 mm depth was reduced to approximately 50% of the original case. This result demonstrates the effectiveness of the proposed technique for transillumination imaging through a diffuse medium. Figure 10 depicts ratios of the widths after subtraction to those before subtraction. The effectiveness of the proposed technique becomes greater at a position that is closer to the incident surface because the change of light propagation path caused by the diffuser addition is larger at positions closer to the incident surface.

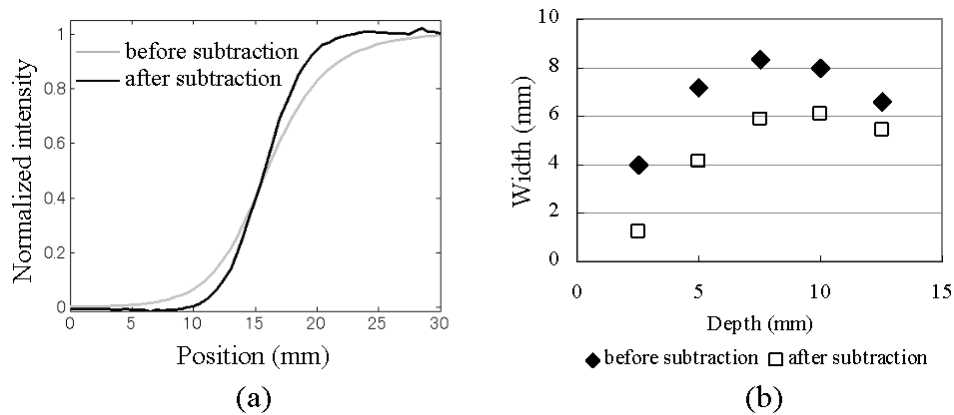


Fig. 9. Results of beam profiling: (a) beam profile at 7.5 mm depth from the front surface, (b) measured width of the propagation area.

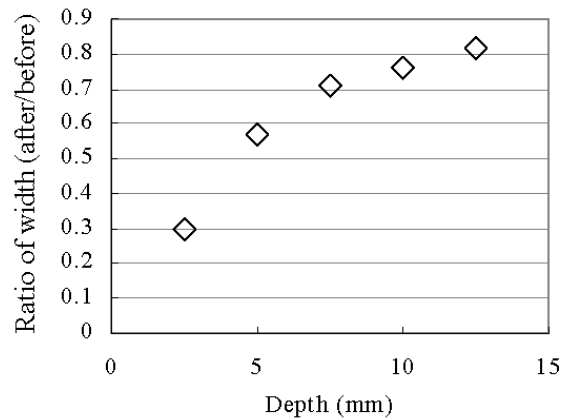


Fig. 10. Width ratios of propagation area before and after subtraction.

5. Application to imaging

5.1 Validity test of the proposed technique for imaging

The validity of the proposed technique for transillumination imaging was tested in an experiment. As a scattering medium, an aqueous solution of Intralipid (reduced scattering coefficient $\mu_s' = 1.0/\text{mm}$) was used in an acrylic resin container with inner wall separation of 30 mm along the optical axis of the incident light beam. As a light source, a detector, and a diffuser, a CW Ti:Sapphire laser (750 nm wavelength), a PIN photodiode, and an opal diffuser were used, respectively. Two black-painted, 2-mm-diameter metallic cylinders were fixed at 15 mm depth in the scattering medium. The distance between the cylinders was 15 mm. Then 2D transillumination images were obtained by scanning the container. An image of the WSL component was obtained using the procedure described in the preceding section. Here, the subtraction weight α was determined as 1.65 according to the ratio of I_1 to I_2 at the position of 15 mm from the optical axis.

Figures 11(a) and 11(b) respectively show transillumination images through the scattering medium with and without a diffuser. Figure 11(c) shows an image of the WSL component obtained using the proposed technique. Figure 12 depicts horizontal average intensity distributions in Figs. 11(a)–11(c). In cases with and without diffuser, the absorbers were not separated in the images. The small WSL component buried in the widely diffused light was extracted, and the absorbers were separated in the image of Fig. 11(c). The contrast of the absorbers was improved about 12 times (from 0.026 to 0.31) using the proposed technique, which suggests that the spatial resolution was improved by extracting the WSL component. These results verify the fundamental validity of the proposed technique for transillumination imaging through a diffuse medium.

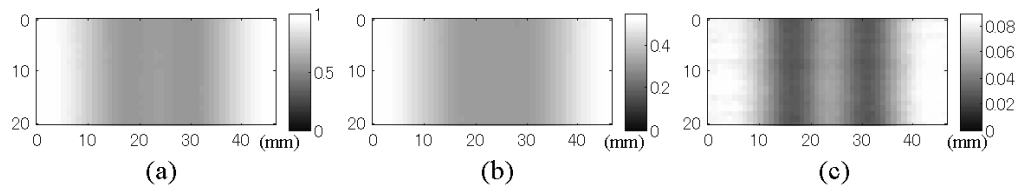


Fig. 11. Images through scattering medium ($\mu_s' L = 30$) with absorbers: (a) without diffuser, (b) with diffuser, (c) subtracted image.

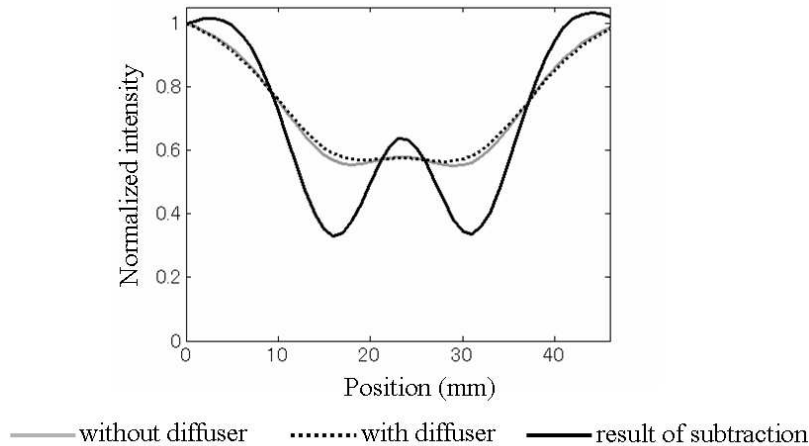


Fig. 12. Intensity distributions of received signal through scattering medium ($\mu_s' L = 30$) with absorbers.

5.2 Imaging through biological tissue

The applicability of the proposed technique to imaging of biological tissues was tested in an experiment. The system and procedure of the measurement were identical to those described in the previous section, except for the following points. As a scattering medium, chicken breast meat was used in an acrylic resin container with inner wall separation of 40 mm along the optical axis of the incident light beam. As an absorber, a black-painted stainless steel plate (9 mm width, 0.3 mm thickness) was fixed at the center of the scattering medium. The subtraction weight α was determined as 2.0 in the manner described previously.

Figure 13(a) depicts a transillumination image taken through the chicken breast meat without a diffuser. Figure 13(b) portrays an image of the WSL component obtained using the proposed technique. The absorber was depicted more clearly using the proposed technique. Viewing Fig. 13(b), the absorber width can be evaluated more exactly. The noisy background in Fig. 13(b) is considered to result from inhomogeneity, such as adipose tissue of the chicken breast meat. The contrast of the image was improved about 1.9 times (from 0.35 to 0.66) using the proposed technique. This result suggests the applicability of the proposed technique to transillumination imaging through a 40-mm-thick biological tissue.

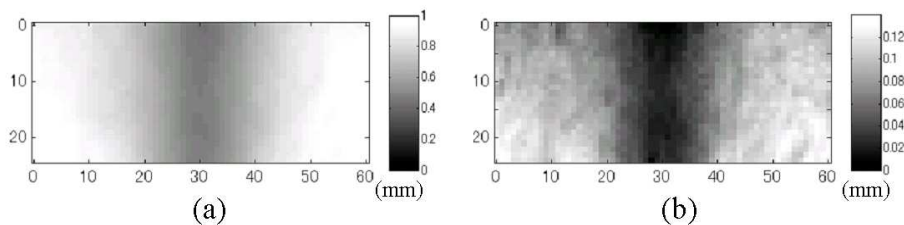


Fig. 13. Images through 40 mm chicken meat with a 9-mm-wide absorber: (a) without diffuser, (b) subtracted image.

6. Application to depth evaluation

We can improve the blurred transillumination image through deconvolution with the depth-dependent point spread function if the depth of an absorber in a scattering medium is available [13]. As described in section 4, the effectiveness of the proposed technique becomes greater as the absorber position approaches the incident surface. We can expect the depth evaluation of absorbers using this characteristic. The possibility of this principle was tested in an experiment.

The measurement system and procedure were identical to those described in section 5.1, except for the following points. As absorbers, two black-painted, 2-mm-diameter metallic cylinders were used. They were fixed at 10 mm and 15 mm, far from the incident surface of the scattering medium with 30 mm thickness. Their interval in a projected plane was 15 mm. The subtraction weight α was determined as 1.66 in the manner described previously. Transillumination images were recorded and the proposed technique was applied. Then, the scattering object was turned 180 deg to reverse the incident and output sides; the same measurement was made.

Figure 14 portrays the contrast improvement ratios of transillumination images made using the proposed technique. With the absorber at 10 mm depth, the contrast improvement ratio differs greatly between the front-incidence case and the rear-incidence case. However, that of the absorber placed at 15 mm depth changed only slightly between the two cases because it was at the center depth. This result suggests that the ratio between the contrast improvement ratio in the front-incidence case and that in rear-incidence case corresponds to the absorber's position in the scattering medium. The depth evaluation can be expected using the ratio.

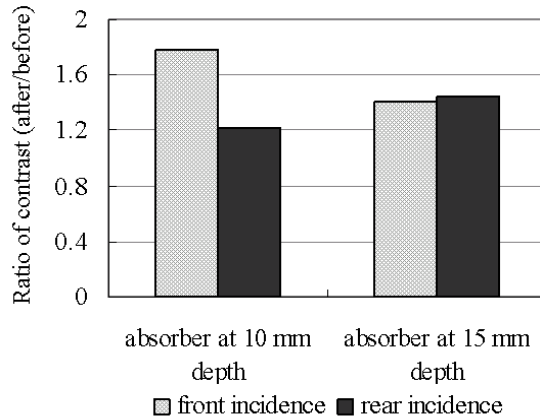


Fig. 14. Improvement ratios of contrast after subtraction in cases of front incidence and rear incidence.

7. Conclusions

With a view toward clear transillumination imaging of an animal body, a new technique was developed to suppress scattering while securing sufficient signal intensity. Using this technique, we can extract a small weakly scattered light component from widely diffused light.

The feasibility of the proposed technique was tested in an experiment. The spatial spread of a light beam was evaluated in CW imaging; the temporal spread of a light pulse was evaluated in time-resolved measurements. In both measurements, the feasibility of the proposed technique to suppress both spreads was verified. The propagation path of the detected light in a scattering medium (15 mm thick, $\mu_s L = 15$) was measured. At 7.5 mm depth, the area of the propagation path was confined to a 50% area around the optical axis using the proposed technique. Results show that the effectiveness of this scattering suppression is depth-dependent. The applicability of the proposed technique to transillumination imaging was examined in experiments with a model phantom and chicken breast meat. With a scattering medium (30 mm thickness, $\mu_s L = 30$), the spatial resolution in the transillumination image was improved and the contrast between the absorbers was improved to about 12 times as large. The 9-mm-wide plate in the center of the 40 mm piece of chicken meat was identified clearly using the proposed technique. As an application of the proposed technique, the possibility of the depth evaluation of an absorber in a diffuse medium was demonstrated.

The proposed technique uses the difference in the degree of diffusion between the cases before and after the attachment of a diffuser. Therefore, we must choose a diffuser that provides a sufficient change in the degree of diffusion. In practice, a thin diffuser plate with a high scattering coefficient is preferred for transillumination imaging of animal bodies with curved surface.

The mean free path of a photon in a general biological tissue is about 1 mm-long. Therefore, clear transillumination imaging was considered impossible with tissues thicker than 10 mm. In such a case, the coherence and polarization of incident light are lost in diffuse scattering, and practical S/N cannot be expected, even in the time-gating technique. The proposed technique does not depend on these optical characteristics. It uses the light that experienced multiple scattering but the diffused area was confined around the optical axis of the incident light beam. This enables transillumination imaging with scattering suppression with a practical S/N.

When a diffuser plate is applied to the scattering medium, the propagation area of diffused light in the medium changes to some extent. This change of propagation area causes the difference in off-axis intensity at the output surface: it influences the subtraction weight.

However, the influence is not large in many cases. Moreover, it can be suppressed by averaging the intensity over some off-axis area. The choice of the position to determine the subtraction weight is still based on an empirical decision. A systematic method of choosing an appropriate position for the weight is a subject for future study.

One practical merit of the proposed technique is that it is useful with simple instrumentation with some scanning mechanisms for 2D imaging. This technique requires only the attachment of a diffuser on an imaging object and the image subtraction process. Furthermore, this technique requires no strict optical axis alignment because strong collimation is not required.

Consequently, the proposed technique provides a useful tool for non-invasive functional imaging of internal organs at depths that were heretofore considered difficult.

Acknowledgment

This research was supported in part by a Grant-in-Aid for Scientific Research from the Japan Society for the Promotion of Science.